

A Multilevel Collision Mitigation Approach—Its Situation Assessment, Decision Making, and Performance Tradeoffs

Jörg Hillenbrand, *Student Member, IEEE*, Andreas M. Spieker, and Kristian Kroschel

Abstract—This paper deals with the problem of decision making in the context of forward collision mitigation system design. The authors present a multilevel collision mitigation (CM) approach that allows a flexible tradeoff between potential benefit and the risk associated with driver acceptability and product liability. Due to its practical relevance, algorithms that allow for an efficient incorporation of both sensor and prediction uncertainties are further outlined. The performance tradeoffs that come along with different parameterizations are investigated by means of stochastic simulations on three dangerous traffic situations, namely 1) rear-end collisions due to an unexpected braking, 2) cutting-in vehicles, and 3) crossing traffic at intersections. The results show that an overly conservative CM system sacrifices much of its potential benefit. However, it is pointed out that the vision of accident-free driving can be achieved only through cooperative driving strategies.

Index Terms—Collision mitigation (CM), decision making, driver assistance, performance analysis, situation assessment.

I. INTRODUCTION

COLLISION mitigation (CM) systems will play a major role in improving traffic safety in the near future. Reducing the number of road accidents is of paramount societal importance, and a growing research effort has been devoted to these driver assistance systems within the last few years [1]. Today, the development is in rapid progress, and the first CM systems have recently been introduced to the premium segment market. Yet, little is published on algorithmic details concerning their decision-making methodologies. Decision making for CM (by braking) systems can be stated as the multiattributive problem to decide under which conditions, with regard to the available information on the surrounding environment and the own vehicle, a CM system should intervene, and if so, at what amount of deceleration, thereby taking into consideration the potential benefit of the system, driver acceptability constraints, as well as product liability risk.

In this paper, we address this decision-making problem and provide efficient algorithms to its solution. The presented multilevel CM approach incorporates both sensor and prediction uncertainties and allows for an intuitive tradeoff between the potential benefit of the system on the one hand and the

associated risk concerning driver acceptability and product liability on the other. We focus on a scenario with one object and no restrictions regarding the drivable area. Although these simplifying assumptions lead to suboptimal system behavior in those traffic situations in which the required criticality for a timely intervention can only be deduced if multiple objects are considered jointly, they are of great practical importance for several reasons. One reason is that tackling this problem in its full generality can become arbitrarily complex due to its multidimensional nature. The computational capacity is, however, limited by the computing power of the electronic control units available for automotive applications. Especially if CM systems are to be widely introduced into the market, their technical integration into existing low-cost hardware is likely to be a requirement. Hence, computationally efficient algorithms capable of real-time operation are needed. Further reasons concern the testability of an actual implementation with reasonable time and effort, as well as the difficulty of judging the reliability of information on complex geometric entities like a drivable area.

This paper is organized as follows: In Section II, we introduce the situation assessment metric used in our CM approach and provide algorithms to its efficient computation. In Section III, we discuss general aspects of CM system design and review related work before we present our approach to the decision-making problem. A brief explanation on how we evaluate and compare the benefit of different CM systems is given in Section IV. In Section V, we identify performance tradeoffs by means of stochastic simulations on three typically dangerous situations. Finally, Section VI presents conclusions from this work.

II. SITUATION ASSESSMENT METRICS

Several situation assessment algorithms for forward CM and collision warning systems have been proposed in the past. They range from rather simple methods, which measure collision risk in terms of time to collision (TTC) [2], predicted minimum distance [3], or required deceleration [4], to complex path planning frameworks inspired by the mobile robotics community, e.g., using elastic bands [5], [6].

Our approach is motivated by the following question: Given the ego vehicle's and the object's current state,¹ a prediction model for the object's future motion, and physical constraints imposed by vehicle dynamics, how much time is left for the

Manuscript received November 22, 2005; revised May 3, 2006, July 21, 2006, and July 27, 2006. The Associate Editor for this paper was A. Eskandarian.

J. Hillenbrand and A. M. Spieker are with DaimlerChrysler AG, 71059 Sindelfingen, Germany (e-mail: joerg.hillenbrand@daimlerchrysler.com; andreas.spieker@daimlerchrysler.com).

K. Kroschel is with the Institut für Nachrichtentechnik, Universität Karlsruhe, 76128 Karlsruhe, Germany (e-mail: kroschel@int.uni-karlsruhe.de).

Digital Object Identifier 10.1109/TITS.2006.883115

¹Throughout this paper, properties and states referring to the vehicle being equipped with the CM system are marked by a corresponding "ego" prefix or subscript, whereas properties and states referring to an (arbitrary) object are marked with the abbreviation "obj."

driver of the ego vehicle to begin a maneuver that circumvents a collision with the object? This remaining time, denoted by time to react (TTR), builds a key element in the proposed decision making, which is discussed in Section III. We believe that the TTR is an adequate metric to assess the criticality of traffic situations since it directly relates to the driver's possible actions—a requirement that is not fulfilled by many other approaches, among them the often cited TTC criterion, which is insensitive to lateral offsets and lateral movements of obstacles, because it assigns the same level of criticality to situations where obstacles can be avoided with a slight braking or steering maneuver and where a collision is practically unavoidable. In contrast to acceleration-based risk metrics, a time-based risk metric like TTR allows for a better incorporation of other typically time-based measures, as, e.g., dead times, reaction times, and prewarning times. For example, we might want to warn a driver a specific time before the CM system would intervene in case the driver would not appropriately react on the issued warning.

Formally, the problem of determining TTR can be stated as follows: Let $\mathbf{u}(t) = (\delta_h(t)\rho(t))^T$ denote the driver's control input signal, consisting of steering wheel angle $\delta_h(t)$ and pedal displacement $\rho(t)$, where $\rho(t) < 0$ corresponds to the brake pedal and $\rho(t) > 0$ to the gas pedal displacement. Let us further subsume all relevant parameters, as, e.g., friction coefficients, in the parameter vector \mathbf{p} . Then, the ego vehicle's future states can be written as

$$\mathbf{x}_{\text{ego}}(t) = \int_0^t \mathbf{f}(\mathbf{x}_{\text{ego}}(0), \mathbf{u}(\tau), \mathbf{p}) d\tau \quad (1)$$

with \mathbf{f} denoting the continuous-time state-space model of the ego vehicle's dynamics. Let $\mathbf{C}_{\text{ego}}(t)$ and $\mathbf{C}_{\text{obj}}(t)$ indicate the ego vehicle's and object's occupied spaces on the (x, y) plane at time t , respectively, which are both a function of their respective states and geometries. Then, TTR is given as the solution to the following:

$$\begin{aligned} \text{TTR} = \max_{t^*} \{t^* \geq 0 | \exists \mathbf{u}(t) : \\ \mathbf{C}_{\text{ego}}(t) \cap \mathbf{C}_{\text{obj}}(t) = \emptyset, \quad \forall t \in (0 \dots t_{\text{max}}]\} \\ \text{subject to} \\ \mathbf{u}(t < t^*) = \mathbf{u}(0) \\ \delta_{h,\min} \leq \delta_h(t) \leq \delta_{h,\max} \\ \dot{\delta}_{h,\min} \leq \dot{\delta}_h(t) \leq \dot{\delta}_{h,\max} \\ \rho_{\min} \leq \rho(t) \leq \rho_{\max} \\ \dot{\rho}_{\min} \leq \dot{\rho}(t) \leq \dot{\rho}_{\max}. \end{aligned} \quad (2)$$

Therein, t^* denotes the time span during which the control inputs of the ego vehicle remain unchanged, as is expressed by the first constraint in (2). The last four constraints in (2) are due to physical saturations of the control inputs as well as their derivatives. t_{max} serves as an equivalent replacement to more intuitive but less accurate goal attainment criteria like, e.g., “until the ego vehicle passes by the object,” and better suits the above formulation. t^* is the variable to be maximized and, hence, represents the “last moment” until the driver of the ego vehicle

must start an appropriate maneuver to avoid a collision with the object. By discretizing the time variable and approximating geometries by sets of circles, (2) could be transformed into a finite-horizon mixed-integer constrained optimal control problem [7]. Although this would yield a quite general formulation that could also deal with multiple objects, the computational burden of these methods is too high for real-time operation.

We therefore decided to approximate TTR using a more direct approach. At least for the considered scenario of one object and no restrictions regarding the drivable area, it is obvious that the later a driver wants to successfully react to an imminent collision danger, the more he or she will be forced to exploit the limits of vehicle dynamics and control inputs. Thus, we can approximate (2) by looking at a small set of selected maneuvers that cover the different types of physical constraints. To be more precise, we will look at four selected maneuvers, i.e., 1) maximum braking, 2) maximum acceleration, 3) minimum radius steering to the left, and 4) minimum radius steering to the right. The remaining reaction times to begin with each of these maneuvers are denoted time to brake (TTB), time to kickdown (TTK), and time to steer (TTS). The derivation of these “base” metrics will be explained in the remainder of this section. To avoid confusion, we stress that our CM approach belongs to the class of “CM by braking” systems, i.e., the system's intervention is restricted to braking, and at no time will an autonomous steering maneuver be employed. Nevertheless, the criticality of a traffic situation must be assessed based on the driver's (unrestricted) possibilities to control the vehicle, which also includes, of course, steering and acceleration maneuvers. From tests performed on a proving ground, we conclude that the presented algorithms provide a reasonable compromise between accuracy and complexity, given the assumptions mentioned in Section I. It is worth mentioning that a numerically robust implementation of these algorithms is nontrivial and requires careful algebraic derivations of all degenerate cases.

A. Scene Representation

The ego vehicle and the object are represented as rectangles on a plane in a curved coordinate system, as depicted in Fig. 1. The object's future motion is modeled by means of a constant acceleration along the curved coordinate axes. This choice of coordinate system and motion model allows for explicit algebraic solutions to most of the base metrics derived in the following. This greatly reduces the computational load compared to more flexible approaches that allow a modeling of more or less arbitrary object motions but require solving highly nonlinear equations or even depend on dynamic simulation. In addition to this, it should be mentioned that even if we considered a motion model with more degrees of freedom, we would still have to decide on its parameterization, i.e., we would have to choose a set of coefficients or a probability distribution on the space of coefficients that define the object's future motion in a deterministic or a probabilistic manner. Such an approach is not only very demanding with regard to the computational load but also with regard to the lack of reliable prior information due to incomplete sensor information and the variability of driver behavior. Thus, it is questionable if this increase in complexity pays off with a noteworthy gain in accuracy. Although many

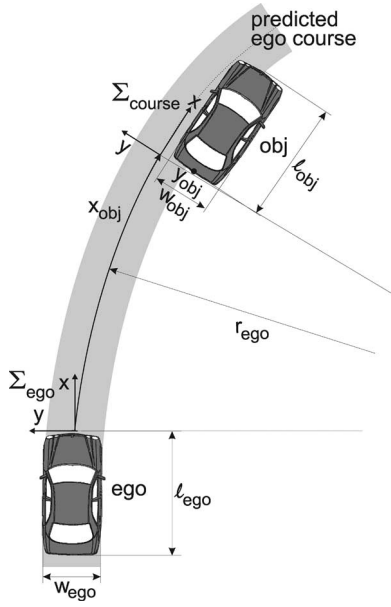


Fig. 1. Object's states are represented in a curved coordinate system Σ_{course} , which follows the ego vehicle's driving corridor. The origin of Σ_{course} coincides with the origin of the Cartesian coordinate system Σ_{ego} , which is attached to the moving ego vehicle.

contributions lead into this direction, as, e.g., [8], our decision-making approach introduced in Section III does not depend on the assumption of a whole probability density for the object's future motion. Instead, it depends only on the “most likely” and the “best case” motion. A constant acceleration model is sufficient for this purpose since it covers those object maneuvers that maximize and minimize our situation assessment metrics. For now, the tracked states are assumed to be exactly known² and given by

$$\mathbf{x}_{obj} = (x_{obj} \ v_{obj} \ a_{obj} \ y_{obj} \ v_{lat} \ a_{lat} \ w_{obj} \ l_{obj} \ c_{obj})^T \quad (3)$$

$$\mathbf{x}_{ego} = (v_{ego} \ a_{ego} \ r_{ego})^T \quad (4)$$

where x_{obj} denotes the object's current longitudinal position; v_{obj} , a_{obj} , v_{ego} , and a_{ego} are the current longitudinal velocities and accelerations of the object and the ego vehicle, respectively; and y_{obj} , v_{lat} , and a_{lat} are the object's lateral position, velocity, and acceleration, respectively. r_{ego} denotes the current driving radius of the ego vehicle, which determines the curvature of the coordinate system, and w_{obj} and l_{obj} denote the dimensions of the object along the (curved) coordinate axes. It should be mentioned that target tracking is usually performed in the Cartesian coordinate system Σ_{ego} , and the corresponding states need to be transformed into the curved coordinate system Σ_{course} first. c_{obj} is an integer state that encodes the object's class (e.g., vehicle type including principal orientation, pedestrian, and nonmoving obstacle) and its physical acceleration limits. Throughout this paper, states without a time argument will refer to a local time $t = 0$ at which the situation is assessed. Constant parameters like width and length of the ego vehicle as well as friction coefficients for straight and circular driving are

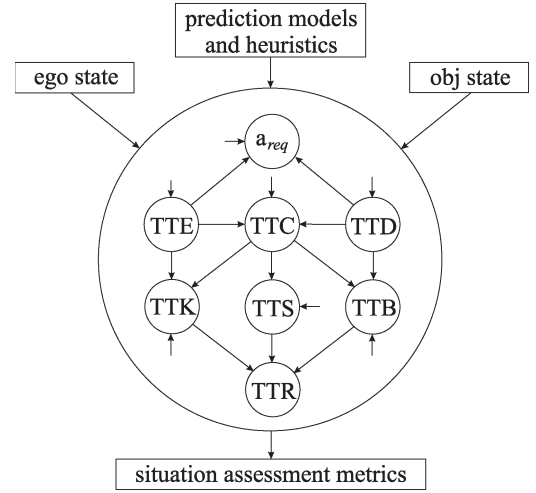


Fig. 2. Information flow at the calculation of the situation assessment metrics.

not regarded as tracked states and are included in an additional parameter vector.

B. Time to Enter (TTE) and Time To Disappear (TTD)

First of all, we determine the time interval $[TTE, TTD]$, $0 \leq TTE < TTD \leq \infty$, in which the object is not completely outside the ego vehicle's driving corridor. Since the object's longitudinal motion is defined along the curved coordinate axis, this reduces to calculating the times when the object crosses the corridor boundaries $y = \pm(w_{ego}/2)$ due to its lateral (perpendicular) motion. Of course, $TTE = 0$ only if the object is already within the corridor, and $TTD = \infty$ if the object remains within, once inside. Besides some special cases for objects whose lateral movement may come to a halt, TTE and TTD are solutions to quadratic equations that are trivial to solve and not explicitly stated here.

C. TTC and TTB

Another important metric is the aforementioned TTC. As illustrated in Fig. 2, TTC serves as an intermediate metric, which is mainly used to simplify the upcoming derivation of TTB, TTK, and TTS. The TTC itself depends on TTE and TTD because a collision exists only if the longitudinal trajectories of the ego vehicle and the object intersect within the interval $[TTE, TTD]$. If this is not the case, there is also no need for the ego vehicle driver to react to anything; thus, $TTR := \infty$. If, however, TTC exists and is of the order of a few seconds, the situation is considered interesting enough to calculate the TTR (respectively TTB, TTK, and TTS). Obviously, $TTR < TTC$ holds; hence, TTC constitutes an upper bound for all these metrics.

TTB denotes the remaining time until an emergency braking at maximum deceleration must be applied to avoid the collision by braking. It depends on TTD because, in situations in which the object cuts out of the ego vehicle's driving corridor, it can be sufficient to “brake through” TTD to avoid the collision instead of decelerating until zero relative velocity is achieved. Accounting for this circumstance as well as for objects that come to a halt renders the derivation of TTB rather lengthy, and we

²Although the effect of sensor uncertainty is not explicitly analyzed in this paper, it is integrated into our decision-making approach in Section III.

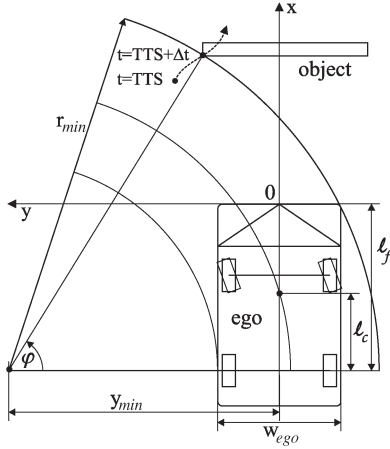


Fig. 3. Avoiding a moving obstacle by a left turn with minimum radius. The turn has to begin at $t = TTS$ such that the ego vehicle's right front corner touches the object's facing left corner somewhere along the circular arc at $t = TTS + \Delta t$.

refer to [9] for a comprehensive statement of algebraic solutions to TTC and TTB.

D. TTS

Let r_{min} denote the minimum possible radius of the ego vehicle's outer front corner at a stationary circular driving with constant track speed (see Fig. 3). Assuming a rectangle-shaped ego vehicle with front steering and rear-wheel drive, r_{min} can be derived as

$$r_{min}(t) = \max \left\{ r_t, \sqrt{l_f^2 + \left(y_{min}(t) + \frac{w_{ego}}{2} \right)^2} \right\} \quad (5)$$

with

$$y_{min}(t) = \max \{ y_t, y_r(t) \}, \quad y_t = \sqrt{r_t^2 - l_f^2} - \frac{w_{ego}}{2} \quad (6)$$

and

$$y_r(t) = \sqrt{\max \left\{ 0, \left(\frac{v_{ego}(t)^2}{\mu_{rt}g} \right)^2 - l_c^2 \right\}} \quad (7)$$

where r_t denotes the ego vehicle's outer turn radius, l_f is the distance from the rear axle to the front bumper, l_c is the distance from the rear axle to the center of gravity, w_{ego} is the width of the ego vehicle, μ_{rt} is the friction coefficient at circular driving, and g is the acceleration of gravity. With $v_{ego}(t) = \max\{0, v_{ego} + a_{ego} * t\}$, r_{min} becomes a function of t . We assume that, at the yet to be determined time $t = TTS$, the driver will stop accelerating and switch the steering angle to drive along the circular arc with minimum radius $r_{min}(TTS)$. Although steering jumps are infeasible for nonholonomic vehicles, this assumption simplifies the upcoming derivation. Furthermore, we could verify by tests that experienced drivers can get very close to such an idealized maneuver.

Our aim is to determine $t = TTS$ such that the ego vehicle's front just passes by the object's facing edges, once the ego vehicle drives along the circular arc. As an obstacle could be avoided by a left turn or a right turn, there will be two—in

general different—values for TTS. However, it is sufficient to derive the solution for a left turn since the solution for a right turn can be deduced from symmetry considerations. Fig. 3 depicts the situation where the ego vehicle has just started to drive along the evasive circular arc. While the ego vehicle is moving along this circular arc with constant track speed, the object keeps moving according to its prediction model. A condition for $t = TTS$ to be the correct solution is that there exists a time $t = TTS + \Delta t$, $\Delta t > 0$, such that the front right corner of the ego vehicle touches the facing left corner of the obstacle at some geometrical point on the circular arc. A solution is guaranteed to exist if 1) it is still possible to avoid the obstacle by a left turn, i.e., it is not too late for that maneuver, and 2) there exists a finite TTC, i.e., action becomes necessary at all. Using a polar coordinate system with its origin fixed at the circular arc's center, a “touching” is achieved by solving the following system of angular and radius equations:

$$\varphi_{obj}(TTS, \Delta t) = \varphi_{ego}(TTS, \Delta t) \quad (8)$$

$$r_{obj}(TTS, \Delta t) = r_{ego}(TTS, \Delta t) = r_{min}(TTS) \quad (9)$$

for the variable TTS. Let $x_{obj}(t)$ and $y_{obj}(t)$ denote the predicted longitudinal and lateral positions of the object's facing left corner along the ego vehicle's current course at time $t \geq 0$, and let $v_{ego}(t) = \max\{0, v_{ego}(0) + a_{ego}(0) * t\}$, $x_{ego}(t) = \int v_{ego}(\tau) d\tau$ denote the ego vehicle's velocity and traveled distance along this course, respectively. The angular equation (8) expands to

$$\begin{aligned} \tan \left(\frac{x_{obj}(TTS + \Delta t) - x_{ego}(TTS) + l_f}{y_{min}(TTS) - y_{obj}(TTS + \Delta t)} \right) \\ = \frac{v_{ego}(TTS)\Delta t}{r_{min}(TTS)} + \arcsin \left(\min \left\{ 1, \frac{l_f}{r_{min}(TTS)} \right\} \right) \end{aligned} \quad (10)$$

and the radius equation (9) becomes

$$\begin{aligned} (x_{obj}(TTS + \Delta t) - x_{ego}(TTS) + l_f)^2 \\ + (y_{min}(TTS) - y_{obj}(TTS + \Delta t))^2 = (r_{min}(TTS))^2 \end{aligned} \quad (11)$$

yielding an implicit coupled nonlinear equation system of the form

$$\mathbf{f}(\mathbf{t}) = \begin{pmatrix} f_1(TTS, \Delta t) \\ f_2(TTS, \Delta t) \end{pmatrix} = \mathbf{0} \quad (12)$$

that needs to be solved iteratively for TTS and Δt , with TTS being the variable of interest. Fortunately, this can be accomplished by a decoupled bisection iteration for each equation, as outlined in the following.

First, we require that TTC is below a least critical value, e.g., 5 s; otherwise, the resulting TTS will be far from any value that can be considered critical. As mentioned before, TTS is upper bounded by TTC since an evasive steering must start before the collision occurs. In a next step, we check whether the steering maneuver is still possible by setting $TTS := 0$ and solving the angular equation (10) for Δt . For every reasonable situation,

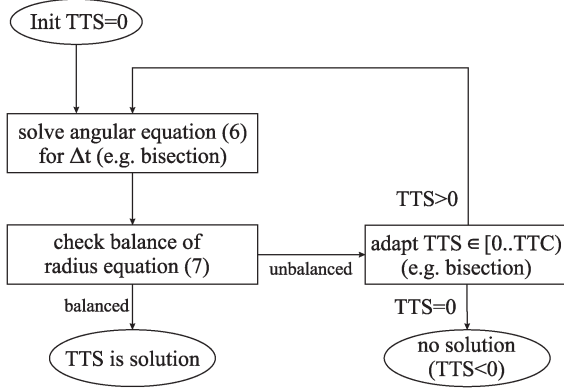


Fig. 4. Iteration scheme for solving TTS for left (respectively, right) turn.

Δt is upper bounded by the time needed for the ego vehicle to reach the 90° angle, i.e.,

$$\Delta t \leq \frac{\pi}{2} \frac{r_{\min}(\text{TTS})}{v_{\text{ego}}(\text{TTS})}. \quad (13)$$

Thus, an “inner” bisection iteration can be used to provide a robust solution to Δt up to any desired accuracy. This solution is plugged into the radius equation (11). If the left-hand side of (11) is greater than its right-hand side—indicating that the ego vehicle passes by without colliding with the object—TTS can be altered in an “outer” bisection iteration until a TTS is found, whose corresponding Δt leads to a balancing of (11). The iteration scheme is illustrated in Fig. 4. Finally, the resulting TTS is obtained by taking the maximum of the respective values for left and right turns, i.e.,

$$\text{TTS} = \max\{\text{TTS}_{\text{left}}, \text{TTS}_{\text{right}}\}. \quad (14)$$

E. TTK

The idea behind this metric is that through acceleration, it might be possible for the ego vehicle to completely pass by the object before it actually enters into the ego vehicle’s driving corridor. An example for such a situation is a slowly driving ego vehicle that will be hit by an intersecting vehicle approaching from the right. In such a situation, it might be sufficient for the driver to push the gas pedal to leave the collision zone early enough. Provided that a TTC exists, TTK is upper bounded by TTE and lower bounded by 0 if a solution exists at all. To avoid the collision

$$x_{\text{ego}}(\text{TTE}) = x_{\text{obj}}(\text{TTE}) + l_{\text{obj}} + l_{\text{ego}} \quad (15)$$

has to be fulfilled. We consider an ego vehicle motion that is switched at $t = \text{TTK}$ from its current longitudinal motion to a motion with maximum acceleration. Noting that $v_{\text{ego}}(\text{TTK}) = \max\{0, v_{\text{ego}} + a_{\text{ego}}\text{TTK}\}$, $x_{\text{ego}}(\text{TTK}) = \int v_{\text{ego}}(\tau) d\tau$, and $a_{\text{ego}}(t \geq \text{TTK}) = h(v_{\text{ego}}(\text{TTK}))$, where h models the acceleration performance of the ego vehicle, it follows that

$$x_{\text{ego}}(\text{TTE}) = x_{\text{ego}}(\text{TTK}) + v_{\text{ego}}(\text{TTK})(\text{TTE} - \text{TTK}) + \frac{1}{2} h(v_{\text{ego}}(\text{TTK})) (\text{TTE} - \text{TTK})^2. \quad (16)$$

Equations (15) and (16) can be solved for TTK using a one-dimensional iteration procedure like the aforementioned bisection method.

F. TTR

The TTR, as stated in (2), can now be approximated by the maximum of the previously derived metrics TTB, TTK, and TTS. Before that, any systematic bias that may result from model simplifications can be compensated, yielding

$$\text{TTR} = \max\{\text{TTB} - b_{\text{TTB}}, \text{TTK} - b_{\text{TTK}}, \text{TTS} - b_{\text{TTS}}\}. \quad (17)$$

In the remainder of this paper, we will not differentiate between the approximated TTR (17) and the original TTR (2) to keep the notation concise.

G. Required Deceleration (a_{req})

The required deceleration a_{req} refers to the constant deceleration that is necessary to just avoid a collision by braking. It will be used as a reference to the controlled deceleration in case of an intervention of the CM system but not as part of an activation criterion. The derivation of a_{req} is based on the fulfillment of $x_{\text{ego}}(t) = x_{\text{obj}}(t)$ together with either the constraint of zero relative velocity $\dot{x}_{\text{ego}}(t) = \dot{x}_{\text{obj}}(t)$ at some common time to touch ($t = \text{TTT}$) or by a switching behavior that determines TTT in case of cutting-out objects or vehicles that come to a standstill. The results are outlined in Figs. 5 and 6.

Since a_{req} does not compensate for the dynamics of the ego vehicle’s brake system, employing an additional controller might improve overall performance. As an example, model reference adaptive control techniques [10] have been successfully applied to various trajectory following problems. In this context, $a_{\text{req}}(t)$ might be used as a reference to the ego vehicle’s desired acceleration response. However, controller design depends on the specific brake system and is beyond the scope of this paper. Furthermore, as will be shown in Section V-A, the determining factor for our test vehicle’s brake system is the pure time delay rather than its first-order time constant. Since a pure time delay could only be compensated by an earlier intervention, the benefit of an additional controller remains very limited in this case.

III. DECISION MAKING UNDER LIABILITY AND DRIVER ACCEPTANCE CONSTRAINTS

The design of a CM system needs to comply with a couple of requirements that result mainly from legal considerations and driver acceptability concerns. For instance, the World Forum for the Harmonization of Vehicle Regulations (Vienna Convention) demands that the driver be in command of the vehicle at all times. This implies that the driver must be able to override an intervention of a CM system, irrespective of the situation at hand. Another important point to consider is protection against misuse. The availability of a CM system should not misguide the driver to intentionally remain passive to let the vehicle automatically handle the situation. A system design that favors such an undesired adaption of driver behavior would obviously be countereffective in terms of traffic safety. In a recent paper [11],

Case 1: The object comes to standstill prior to the collision avoiding touch (TTT) and does not leave the predicted ego corridor until that event.

$$a_{req} = -\frac{a_{obj}v_{ego}^2}{2x_{obj}a_{obj} - v_{obj}^2} \quad (18)$$

$$TTT = -\frac{a_{req}}{v_{ego}} \quad (19)$$

Case 2: The object comes to standstill but disappears thereafter from the predicted ego corridor. This case is relevant for turning or crossing vehicles. The ego vehicle does not need to halt, but needs to make sure that it passes by not until the object has left the (potential) collision zone.

$$a_{req} = \frac{2x_{obj}}{TTD^2} + \frac{v_{obj}^2}{a_{obj}TTD^2} - \frac{2v_{ego}}{TTD} \quad (20)$$

$$TTT = TTD \quad (21)$$

Case 3: The object disappears from the predicted ego course during its regular motion, i. e. before it comes to a possible halt. Again, the ego vehicle does not necessarily need to attain the object's velocity.

$$a_{req} = a_{obj} + \frac{2(v_{obj} - v_{ego})}{TTD} + \frac{2x_{obj}}{TTD^2} \quad (22)$$

$$TTT = TTD \quad (23)$$

Case 4: The object neither comes to standstill nor disappears from the ego vehicle's driving corridor until the collision avoiding touch (TTT). This corresponds to the regular case.

$$a_{req} = a_{obj} - \frac{(v_{obj} - v_{ego})^2}{2x_{obj}} \quad (24)$$

$$TTT = -\frac{2x_{obj}}{v_{obj} - v_{ego}} \quad (25)$$

Fig. 5. Different cases for the derivation of the required deceleration a_{req} .

a sufficiently large stochastic variation of activation thresholds has been proposed to mitigate negative behavioral adaption. However, we expect that reasonably chosen static thresholds will not lead to interventions frequent enough to allow for a behavioral adaption. Furthermore, intentional misuse can be prevented by limiting the amount of interventions to about one or two during one ignition run and displaying a corresponding message to the driver in case this limit is exceeded.

Apparently, requirements like the above mentioned can be incorporated into a CM system by adding some extra functionality to it. However, the main question remains yet to be clarified: When, i.e., under which conditions, do we want the CM system to intervene, and if so, what amount of deceleration should be applied? Unfortunately, there seems to be no “optimal” answer to this kind of question. The reason is that optimality (in a strictly scientific manner) first requires the definition of an optimal reference to which the actual performance can be compared against, e.g., in a least mean squared error sense. In a dynamic nondeterministic environment with incomplete sensor information, fuzzy driver acceptance constraints, and unsettled liability issues, an optimal reference model, however, hardly exists. Consequently, different approaches have been proposed in literature with differing situation assessment metrics and decision-making methodologies.

Step 1: Check for numerically problematic input data to avoid divisions by zero and restrict the calculation of a_{req} to meaningful situations with positive x_{obj} , v_{ego} , v_{obj} , TTD and finite TTE.

Step 2: Calculate a_{req} using the equations in Fig. 5 together with the following algorithm:

```

if  $v_{ego} > v_{obj}$  then
     $a_{req} := (24)$ ;  $TTT := (25)$ ;
else
     $a_{req} := 0$ ;  $TTT := \infty$ ;
end
if  $a_{obj} < 0$  then
    if  $TTD < \min(-\frac{v_{obj}}{a_{obj}}, TTT)$  then
         $a_{req} := (22)$ ;
    end
    if  $-\frac{v_{obj}}{a_{obj}} \leq \min(TTD, TTT)$  then
         $a_{req} := (18)$ ;  $TTT := (19)$ ;
        if  $TTT > TTD$  then
             $a_{req} := (20)$ ;
        end
    end
end
else
    if  $TTT > TTD$  then
         $a_{req} := (22)$ ;
    end
end
end

```

Fig. 6. Outline of the algorithm for the calculation of a_{req} .

In [4], a CM system is considered, which performs only late braking to reduce the collision speed. The authors use an acceleration-based metric and propose a statistical hypothesis test, taking into account all the state uncertainties that arise from target tracking by means of a Monte Carlo integration. In [12], a systematic method to threshold placement for collision warning systems is introduced based on a generalized state-space alerting theory. In essence, the method relies on the definition of trajectory distributions that model the outcomes for the possible actions the system can take. Once these distribution functions are determined, decision boundaries can be derived, which optimally trade off along the system operating characteristic curve. Besides the considerable computation time, the main drawback of these probabilistic approaches is to rely on distributions that—at the utmost—roughly reflect the real world. The short-term models used for target tracking, and likewise the corresponding state densities, may be an inappropriate choice to predict the behavior of the tracked object for the next couple of seconds. In practice, it may be even too difficult to find accurate models for the measurement noise, e.g., when complex image processing algorithms are used, which contain lots of heuristics and depend on other unobservable factors. To take this argument a bit further, we point out that the future behavior of other traffic participants is not even independent of our own “being there.” Other road users might change their behavior if they are aware of the approaching ego vehicle. This is in particular true for oncoming traffic, intersection-like situations, and pedestrians crossing the road: Oncoming drivers may steer aside to create some free space in the middle of the road for the ego vehicle to pass through, intersecting drivers may suddenly brake to avoid crossing the intersection at all,

and pedestrians may step back or start running to leave the potential collision zone. This raises the question if probabilistic techniques provide an appropriate modeling of this problem at all [13]. In [14], the concept of satisficing³ as a human-centered decision-making paradigm is introduced to collision avoidance system design and applied to a lane departure prevention system. Although this concept appears to be more suited to the problem, the required definition of utility and cost functions (therein termed “accuracy” and “liability functions”) is somewhat problematic in the context of a CM system. What is the utility of not colliding with an object or colliding at reduced speed or reduced kinetic energy? In addition, to what extent does the value of utility change if we take additional information on the type of object into account? Obviously, many definitions fulfilling certain monotonicity constraints could be considered reasonable.

We propose a more practical approach that is of much lower complexity but at the same time facilitates a flexible parameterization of the CM system. Consider a multilevel CM system with m active levels, where the levels $i = 1, \dots, m$ correspond to an increasing confidence about the criticality of the situation. $i = 0$ denotes the inactive level where no autonomous braking is performed. Each level i is defined by three threshold values, i.e.,

$$\mathcal{L}^i \triangleq \{\lambda_{\text{mod}}^i, \lambda_{\text{max}}^i, a_{\text{lim}}^i\}, \quad i = 0, \dots, m \quad (26)$$

subject to

$$\lambda_{\text{mod}}^i > \lambda_{\text{mod}}^j, \lambda_{\text{max}}^i > \lambda_{\text{max}}^j, a_{\text{lim}}^i \geq a_{\text{lim}}^j, \quad \text{for } i < j \quad (27)$$

with $\lambda_{\text{mod}}^0 = \lambda_{\text{max}}^0 = \infty$, $a_{\text{lim}}^0 = 0$, and $\lambda_{\text{max}}^i \geq \lambda_{\text{mod}}^i$, i.e., the thresholds are (strictly) monotonically decreasing with respect to level i . λ_{mod}^i and λ_{max}^i are thresholds for TTR_{mod} and TTR_{max} , as explained in the following. Each level's deceleration is limited to a_{lim}^i , i.e., level i is not allowed to autonomously brake with a deceleration of higher magnitude. The criticality of the situation is measured in terms of TTR as derived in Section II. We denote by TTR_{mod} the expected TTR. TTR_{mod} results from the current state vector estimate $\hat{\mathbf{x}}_{\text{aug}}$ and additional heuristics, with which we try to model the “most likely” future behavior of the object in question. As an example, one such heuristic concerns the cutting-in behavior of vehicles driving in the same direction than the ego vehicle. Just because an object's lateral velocity estimate indicates a cutting-in, that does not necessarily mean that the corresponding TTE estimate should be accepted as the most likely one. If the tracked lateral velocity is very inaccurate, e.g., due to the limitations of the sensor system, it might be necessary to completely reject this information to achieve a reasonable system behavior. However, even if the lateral states are tracked with high accuracy, a reliable early recognition of cutting-in vehicles [15] requires additional information like lane markings to avoid frequent false alarms due to seemingly cutting-in vehicles.

Although TTR_{mod} can be considered a likely estimate of the criticality in general, it is still subject to sensor and pre-

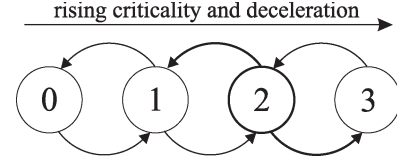


Fig. 7. Three-level CM system where level $i = 2$ is currently the active level. The arrows indicate the transitions to neighboring levels. The system jumps into level 1 as soon as the (signed) required deceleration rises above the deceleration limit of level 1. Level 3 becomes the active level only if the criticality exceeds the necessary confidence for level 3 and level 2 cannot provide the required deceleration.

diction uncertainties. We account for these uncertainties by incorporating the maximum TTR, denoted TTR_{max} , into our decision making. How to efficiently determine TTR_{max} will be discussed in Section III-B; as for now, assuming that TTR_{max} is a known value improves the ease of read. Let $k(n-1)$ denote the set level of the last time step. At every time step n , we select the levels k^{inc} and k^{dec} fulfilling the following threshold comparisons:

$$\begin{aligned} k^{\text{inc}} &= \max \{i \mid (\text{TTR}_{\text{mod}} \leq \lambda_{\text{mod}}^i) \wedge (\text{TTR}_{\text{max}} \leq \lambda_{\text{max}}^i)\} \\ k^{\text{dec}} &= \min \{i \mid (a_{\text{req}} \geq a_{\text{lim}}^i)\}. \end{aligned} \quad (28)$$

In words, k^{inc} selects the highest feasible level with regard to criticality, and k^{dec} selects the lowest level necessary to provide the required deceleration. The new level $k(n)$ is then set to

$$k(n) = \min \{k^{\text{dec}}, \max \{k^{\text{inc}}, k(n-1)\}\} \quad (29)$$

and the (signed) deceleration demanded from the ego vehicle's brake system is, at every instance, given by

$$a_{\text{set}}(n) = \max \{a_{\text{req}}, a_{\text{lim}}^{k(n)}\} \quad (30)$$

with a_{req} being the required deceleration as stated in Fig. 6. Experiments in our test vehicle showed a fairly satisfying closed-loop behavior of this purely predictive control scheme, and no additional controller was implemented. The transition (29) yields a favorable hysteresis effect: Once the CM system jumps into a certain level, it will not decrease its level until the situation relaxes, insofar as a lower level can take over with respect to the required deceleration. On the other hand, it will only increase its level (again) if the criticality reaches the required confidence of the following level and the current level cannot provide the required deceleration. Fig. 7 illustrates the case of a three-level CM system. It is worth mentioning that a first “warning only” level could be easily included into this scheme by setting $a_{\text{lim}}^1 := 0$.

A. Parameterization of the CM System

Parameterization of the CM system corresponds to choosing the number of active levels m as well as their respective thresholds \mathcal{L}^i . λ_{mod}^i and a_{lim}^i are the main parameters with which we can trade off driver acceptance, liability, and potential benefit of the system. λ_{max}^i primarily safeguards the decision for level i against sensor and prediction uncertainties. The higher the level, and thus the allowed deceleration, the more we might want to make sure that the situation indeed shows the

³The term satisficing is a cross between “satisfying” and “sufficing.” The concept aims at obtaining an outcome that is good enough rather than an optimal solution for demanding optimality may lead to ill-formed problems due to lack of information or resources.

required criticality and will maintain it—even if the obstacle changes its motion. However, a decrease in λ_{\max}^i will also result in a decrease of benefit. As a starting point, consider a system with $m = 2$ active levels. The first level shall perform an early braking with an unproblematic deceleration, while the second level shall perform a late braking at maximum deceleration to reduce collision severity. The system must be parameterized such that it will be accepted by a high majority of drivers. This implies that the first level must not activate too early with respect to TTR_{mod} . Furthermore, its deceleration should be limited to a magnitude that will neither strain the driver too much in case of an undesired activation nor raise liability questions regarding rear traffic, which might crash into the ego vehicle due to its autonomous braking. To activate the second level, we require that a collision will occur under any circumstances. Ensuring this should vitiate any liability concerns. One possible parameterization of this two-level CM system is given by

$$\begin{aligned}\mathcal{L}^1 &\triangleq \{2.0 \text{ s}, 5.0 \text{ s}, -3.0 \text{ m/s}^2\} \\ \mathcal{L}^2 &\triangleq \{0.0 \text{ s}, 0.0 \text{ s}, -\infty \text{ m/s}^2\}.\end{aligned}\quad (31)$$

As we did not include some kind of utility or benefit measure into our decision-making approach so far, we cannot tell *ad hoc* how the benefit of the CM system changes quantitatively when parameters are modified or intermediate levels are added. This of course depends on the type of situation itself and on how we measure benefit at all. Once these questions are settled, we can simulate different alternatives until a parameterization is found that best reflects the carmaker's preferences.

B. Determining TTR_{max}

Our aim is to determine the TTR of the least critical situation that is possible with respect to sensor and prediction uncertainties. Noteworthy sensor uncertainties arise predominantly in the tracked object states and the friction coefficients. States related to the ego vehicle are usually measured with high accuracy and henceforth shall be considered as perfectly known. We introduce the abbreviation x^\pm to indicate the upper (respectively lower) limit of a (scalar) tracked object state due to its sensor uncertainty. For a Gaussian uncertainty, as is the case for Kalman filter-based target tracking [16], we suggest using the 3σ limits, i.e., $x^\pm = \hat{x} \pm 3\sigma_x$. In case the target is tracked with a nonlinear state-space estimation technique like the particle filter [17], setting x^\pm to the (marginalized) distribution's support limits yields a conservative estimate. If we neglect the possibility that a nonstationary obstacle could change its acceleration at any time, we can replace the respective state components of $\hat{\mathbf{x}}_{\text{aug}}$ by the components of the following two vectors:

$$\mathbf{x}_{\text{rep}}^+ = \left(l_{\text{obj}}^- w_{\text{obj}}^- \mu_r^+ \mu_{\text{rt}}^+ x_{\text{obj}}^+ v_{\text{obj}}^+ a_{\text{obj}}^+ y_{\text{obj}}^+ v_{\text{lat}}^+ a_{\text{lat}}^+ \right)^T \quad (32)$$

$$\mathbf{x}_{\text{rep}}^- = \left(l_{\text{obj}}^- w_{\text{obj}}^- \mu_r^+ \mu_{\text{rt}}^+ x_{\text{obj}}^+ v_{\text{obj}}^+ a_{\text{obj}}^+ y_{\text{obj}}^- v_{\text{lat}}^- a_{\text{lat}}^- \right)^T. \quad (33)$$

Replacing the corresponding components of $\hat{\mathbf{x}}_{\text{aug}}$ according to (32) and (33) yields two test particles, which model an obstacle that “escapes” into the forward-left and forward-right directions, respectively. One of these test particles will maximize

TTR due to monotonicity properties.⁴ Now, we shall drop the assumption that the object follows the constant acceleration model. We denote by a_{obj}^{\max} , a_{lat}^{\min} , and a_{lat}^{\max} the object's (signed) maximum possible longitudinal acceleration, its minimum possible lateral acceleration, and its maximum possible lateral acceleration, respectively. Clearly, these values are only estimates that depend on the type of object, its orientation with respect to our curved coordinate system, its velocity, and other factors like friction coefficients. Since a nonstationary object can change its acceleration discontinuously and instantly, we can simply replace the respective accelerations in (32) and (33). Hence, the state components that approximately maximize TTR are contained within the following set:

$$\begin{aligned}\mathbf{x}_{\text{rep}}^+ \left(a_{\text{obj}}^+ a_{\text{lat}}^+ \right) &\leftarrow \left(\max \left\{ a_{\text{obj}}^+, a_{\text{obj}}^{\max} \right\} a_{\text{lat}}^+ \right) \\ \mathbf{x}_{\text{rep}}^+ \left(a_{\text{obj}}^+ a_{\text{lat}}^+ \right) &\leftarrow \left(a_{\text{obj}}^+ \max \left\{ a_{\text{lat}}^+, a_{\text{lat}}^{\max} \right\} \right) \\ \mathbf{x}_{\text{rep}}^+ \left(a_{\text{obj}}^+ a_{\text{lat}}^+ \right) &\leftarrow \left(\max \left\{ a_{\text{obj}}^+, \frac{a_{\text{obj}}^{\max}}{\sqrt{2}} \right\} \max \left\{ a_{\text{lat}}^+, \frac{a_{\text{lat}}^{\max}}{\sqrt{2}} \right\} \right) \\ \mathbf{x}_{\text{rep}}^- \left(a_{\text{obj}}^+ a_{\text{lat}}^- \right) &\leftarrow \left(\max \left\{ a_{\text{obj}}^+, a_{\text{obj}}^{\max} \right\} a_{\text{lat}}^- \right) \\ \mathbf{x}_{\text{rep}}^- \left(a_{\text{obj}}^+ a_{\text{lat}}^- \right) &\leftarrow \left(a_{\text{obj}}^+ \min \left\{ a_{\text{lat}}^-, a_{\text{lat}}^{\min} \right\} \right) \\ \mathbf{x}_{\text{rep}}^- \left(a_{\text{obj}}^+ a_{\text{lat}}^- \right) &\leftarrow \left(\max \left\{ a_{\text{obj}}^+, \frac{a_{\text{obj}}^{\max}}{\sqrt{2}} \right\} \min \left\{ a_{\text{lat}}^-, \frac{a_{\text{lat}}^{\min}}{\sqrt{2}} \right\} \right)\end{aligned}\quad (34)$$

where “ \leftarrow ” denotes the replacement operator. Thus, a reasonable approximation to TTR_{max} requires the propagation of merely six selected test particles through the function (17) and selecting the maximum.

IV. PERFORMANCE MEASURES AND ANALYSIS OF FORWARD CM SYSTEMS

As mentioned before, it is necessary to define the benefit of a CM system to identify fundamental tradeoffs and find an acceptable parameterization. Besides warning the driver, which is not considered here, the CM system's only action that has a “direct” influence on the situation is braking. We compare each parameterization against a standard ego vehicle being not equipped with any CM system at all by means of a stochastic simulation and propose the following performance measures.

- The “reaction time gain” ΔTTR . ΔTTR denotes the amount of time that the ego driver gains due to the autonomous braking of the CM system (compared to the standard vehicle) until the ego vehicle reaches $TTR = 0$ in both cases. If the CM system avoids an otherwise happening collision all by itself, ΔTTR is undefined.
- The “collision velocities” $\mathbf{v}_{\text{col}} = (v_{\text{col}}^{\text{STD}}, v_{\text{col}}^{\text{CMS}})^T$ for standard and CMS ego vehicle, respectively. v_{col} denotes the magnitude of the vectorial relative speed at collision time, i.e., at $TTC = 0$. From \mathbf{v}_{col} , the reduction in collision speed $\Delta v_{\text{col}} = v_{\text{col}}^{\text{STD}} - v_{\text{col}}^{\text{CMS}}$ is calculated. Energy- or injury-based performance measures could also be derived

⁴In cases where it is possible to pass by the object before it enters into the ego vehicle's driving corridor (see Section II-E), it is necessary to check for the backward-left and backward-right directions as well.

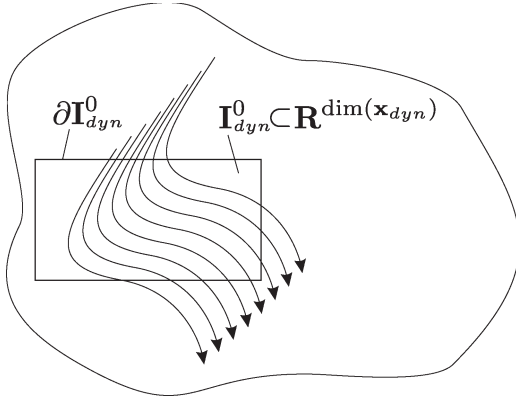


Fig. 8. Dynamic components of the initial states must be sampled uniformly on the initial space's surface to yield an equal weighting of all trajectories that traverse from the outside area into the inside area.

from \mathbf{v}_{col} but requires further knowledge of object type and mass.

- The probability that a collision is avoided due to the autonomous braking of the CM system.

We pose the following question: What benefit, in terms of the above definitions, can we expect from a certain CMS parameterization? Of course, the benefit depends on the sensor system and the acceleration limits of the particular object. However, in the first instance, it depends on the very situation itself, i.e., on the true state vector $\mathbf{x}_{aug}^0 := \mathbf{x}_{aug}(t=0)$, which constitutes the initial state for the dynamic progression of the ego vehicle and the object. Since we have no reliable prior information on the frequency of different traffic situations, a coarse averaging over all traffic situations yields no reasonable benchmark. We get around this difficulty by partitioning the situation space into disjoint situation classes, where each class contains qualitatively similar situations and models a certain use case. This has the additional advantage to point out those use cases where the performance differences between different parameterizations are big or small. Each situation class is subject to a separate performance analysis by means of a Monte Carlo simulation: At first, we sample from the initial space $\mathbf{I}^0 \subset \mathbb{R}^{\dim(\mathbf{x}_{aug})}$, which defines the considered situation class. Then, each sample $\mathbf{x}_{aug}^0 \in \mathbf{I}^0$ serves as an initial state for two dynamic simulations incorporating either the standard ego vehicle or the CMS ego vehicle together with the object. Each dynamic simulation stops whenever it comes to a collision or the simulation time reaches its sufficiently chosen maximum. In a final step, statistics of the performance measures are estimated for each parameterization and each situation class.

It is worth mentioning that sampling the initial states is not straightforward if we seek an equal weighting of every dynamic situation contained within the initial space. To point this out, we separate the initial space into a static and a dynamic part, i.e., $\mathbf{I}^0 = \mathbf{I}_{sta}^0 \cup \mathbf{I}_{dyn}^0$. \mathbf{I}_{sta}^0 denotes the subspace of those initial states that remain constant throughout one dynamic simulation, e.g., w_{obj}^0 and μ_r^0 . These initial states are sampled independently using a uniform distribution. On the other hand, \mathbf{I}_{dyn}^0 denotes the subspace of those initial states that change dynamically during one simulation, e.g., x_{obj}^0 and v_{ego}^0 . These states are sampled uniformly from the boundary $\partial \mathbf{I}_{dyn}^0$ to achieve an equal weighting of all trajectories that enter into

TABLE I
INITIAL SPACES OF THREE SITUATION CLASSES

States	Sit. Class 1	Sit. Class 2	Sit. Class 3
v_{ego}^0	$\mathcal{U}(11, 17)$	$\mathcal{U}(35, 45)$	$\mathcal{U}(11, 17)$
a_{ego}^0	$\mathcal{U}(-0.2, 0.2)$	$\mathcal{U}(-0.2, 0.2)$	$\mathcal{U}(-0.5, 0.5)$
x_{obj}^0	$\mathcal{U}(30, 40)$	$\mathcal{U}(30, 50)$	$\mathcal{U}(10, 20)$
v_{obj}^0	$\mathcal{U}(5, 8)$	$\mathcal{U}(22, 25)$	$\mathcal{U}(-\varepsilon, \varepsilon)$
a_{obj}^0	$\mathcal{U}(-10, -6)^1$	$\mathcal{U}(-0.2, 0.2)$	$\mathcal{U}(-\varepsilon, \varepsilon)$
y_{obj}^0	$\mathcal{U}(-0.5, 0.5)$	$\mathcal{U}(-3.3, -3.6)$	$\mathcal{U}(-3, -8)$
v_{lat}^0	$\mathcal{U}(-\varepsilon, \varepsilon)$	$\mathcal{U}(-\varepsilon, \varepsilon)$	$\mathcal{U}(3, 17)$
a_{lat}^0	$\mathcal{U}(-\varepsilon, \varepsilon)$	$\mathcal{U}(0.5, 1.1)^2$	$\mathcal{U}(-0.2, 0.2)$
w_{obj}^0	$\mathcal{U}(1.65, 1.85)$	$\mathcal{U}(2.10, 2.50)$	$\mathcal{U}(3.8, 5.1)$
l_{obj}^0	$\mathcal{U}(3.8, 5.1)$	$\mathcal{U}(8, 12)$	$\mathcal{U}(1.65, 1.85)$
μ_r^0	$\mathcal{U}(0.8, 1)$		
μ_{rt}^0	$\mathcal{U}(0.7, 0.8)$		

¹values are limited to $\pm \mu_r g$.

²using the lane change model (36).

the initial space. Drawing the samples from \mathbf{I}_{dyn}^0 would yield a skewed boundary distribution, which is dependent on how the trajectories contract or expand within the volume. This behavior is illustrated in Fig. 8 on a two-dimensional example.

V. SIMULATION RESULTS

In this section, we will briefly analyze the performance of two differently parameterized CM systems, namely 1) the rather “cautious” two-level system as previously described in (31) and 2) a more “ventured” three-level system, which is parameterized as follows:

$$\begin{aligned}
 \mathcal{L}^1 &\triangleq \{2.0 \text{ s}, \infty \text{ s}, -4.0 \text{ m/s}^2\} \\
 \mathcal{L}^2 &\triangleq \{0.8 \text{ s}, 3.0 \text{ s}, -6.0 \text{ m/s}^2\} \\
 \mathcal{L}^3 &\triangleq \{0.0 \text{ s}, 0.3 \text{ s}, -\infty \text{ m/s}^2\}. \quad (35)
 \end{aligned}$$

Due to limited space, we will not consider any particular sensor system. There exists a variety of sensor systems differing in field of view, measurement quality, and tracking algorithm, and a thorough investigation of their pros and cons in different situation classes is clearly beyond the scope of this paper. Instead, we focus on a general demonstration and assume a perfect sensor system, i.e., the following results account only for the prediction uncertainty. We investigate the performance of both CMS parameterizations on the three situation classes summarized in Table I. Therein, $\mathcal{U}(a, b)$ denotes a uniform distribution within the interval $[a, b]$.

Situation class 1 describes an ego vehicle at city-like speed, which approaches a rather slow passenger car moving within the same straight line. With respect to their relative velocity, the distance is clearly too small to be considered safe. However, the true TTR is still above 2 s. Suddenly, the object vehicle brakes unexpectedly hard with constant deceleration until it comes to a standstill.

Situation class 2 characterizes an ego vehicle driving on a highway at typical highway-like speed. A much slower truck is driving on the neighboring right lane. As the ego vehicle is just about to overtake, the truck cuts in. The truck's lane

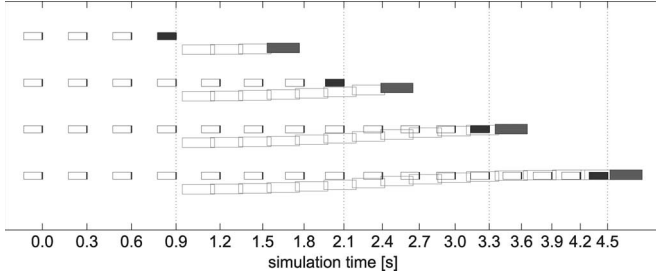


Fig. 9. Snapshots of a cutting-in maneuver from situation class 2. The ego vehicle is equipped with the three-level CM system given by the parameterization (35). The collision has been avoided due to the autonomous braking.

change is modeled using a piecewise-defined constant lateral acceleration, i.e.,

$$a_{\text{lat}}(t) = \begin{cases} +a_{\text{lat}}^0, & t = [0, \frac{T}{2}] \\ -a_{\text{lat}}^0, & t = [\frac{T}{2}, T] \\ 0, & t > T \end{cases} \quad \text{with } T = \sqrt{\frac{4\Delta y}{a_{\text{lat}}^0}} \quad (36)$$

where T denotes the required lane change time, and Δy is the lateral lane change distance, which is set to $|y_{\text{obj}}^0|$ to achieve a lateral end position in line with the ego vehicle. This model yields a symmetric lane change maneuver that approximates the experimentally proven model given in [18].

Situation class 3 models a general intersection situation. The ego vehicle approaches an intersection at common city speed while a passenger car is crossing this intersection from the right-hand side. We assume that the object is not visible beyond a lateral offset of 8 m due to the typical occlusions within cities. Since we focus on forward CM systems, the minimum longitudinal distance is set to 10 m to distinguish the situation class from a side-impact scenario.

We assume a normal friction coefficient for all three situation classes according to Table I. Furthermore, the ego vehicle's parameters are chosen to approximate our test vehicle, i.e., a Mercedes E-class 320, and we assume the same acceleration capabilities for the passenger car in situation classes 1 and 3. For situation class 2, we assume a truck vehicle that has—at the given speed—no further longitudinal acceleration capabilities but a deceleration capability of -6 m/s^2 . Its lateral acceleration capability is assumed to be $\pm 1.5 \text{ m/s}^2$. There is no specific driver model implemented into the simulation environment. Instead, we assume that the driver of the ego vehicle remains passive throughout the simulation. Thus, the only change in the ego vehicle's dynamics is due to an intervention of the CM system. Since we are interested in the potential benefit of the CM system (which virtually implies the assumption of an inattentive driver), the lack of an appropriate driver model is of no disadvantage.

A. Example of the Control Behavior

To provide a better understanding of our CM system approach, its overall control behavior is demonstrated on an example from situation class 2 where the ego vehicle is equipped with the three-level CM system (35). Fig. 9 illustrates the dynamic progression of this cutting-in situation, and Fig. 10 shows the corresponding situation assessment and deceleration

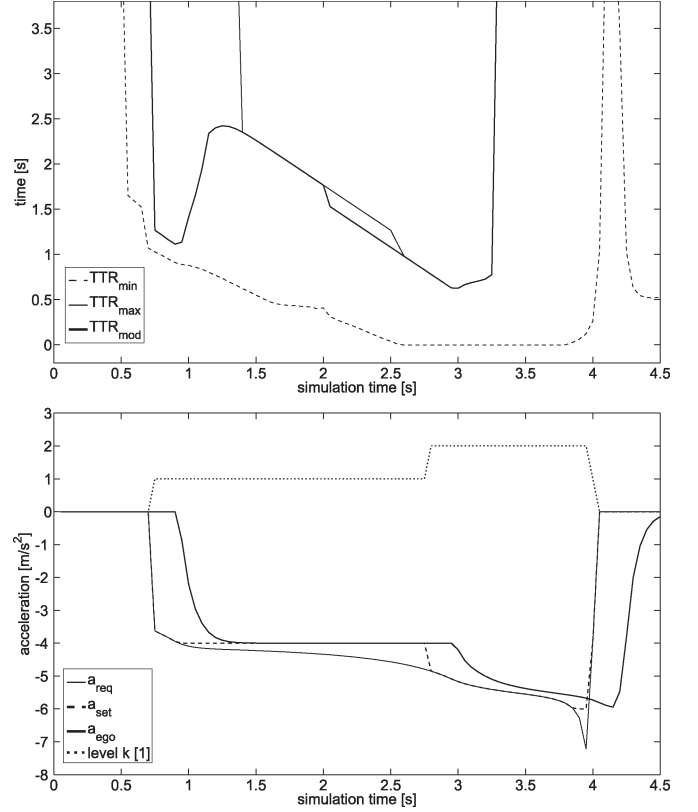


Fig. 10. Upper: Estimates of the minimum, the mode, and the maximum TTR. The minimum TTR corresponds to a worst case behavior of the object and is not used in our decision making. This is reasonable since many real-world traffic situations, as, e.g., oncoming traffic and overtaking scenarios, can become arbitrarily critical if we assume that the object intends to collide with the ego vehicle. Lower: Required deceleration, level-dependent set deceleration of the CM system, and actual deceleration of the ego vehicle due to the brake system's dynamics (modeled as a first-order system with a pure time delay of 0.14 s and a time constant of 0.08 s).

TABLE II
ESTIMATED COLLISION PROBABILITIES (IN PERCENT)

Simulation	$\Pr(\bar{C}, \bar{S})$	$\Pr(\bar{C}, S)$	$\Pr(C, S)$	$\Pr(\bar{C} S)$	$\Pr(\bar{C} S)^*$
Sit. Class 1					
2-Level	0.00	0.00	100.00	0.00	0.00
3-Level	0.00	94.32	5.68	94.32	99.52
Sit. Class 2					
2-Level	0.52	1.24	98.24	1.25	4.78
3-Level	0.44	29.60	69.96	29.73	34.11
Sit. Class 3					
2-Level	61.24	0.00	38.76	0.00	0.00
3-Level	60.96	6.44	32.60	16.50	16.70

* assumes that the ego vehicle driver avoids the collision in case the CM system provides a reaction time gain of 1s or more.

signals. After 0.75 s from the beginning of the simulation, the cutting-in of the truck vehicle is recognized as such, and TTR_{mod} drops from infinity to 1.27 s, which results in the activation of the CM system's first level. The set deceleration equals the required deceleration since the latter does not exceed the first level's limit of -4 m/s^2 . However, due to the brake system's time delay, there is no immediate feedback to the ego vehicle's deceleration, and TTR_{mod} keeps falling linearly with an angle of -45° . As a consequence of this time delay, the required deceleration does not remain constant and

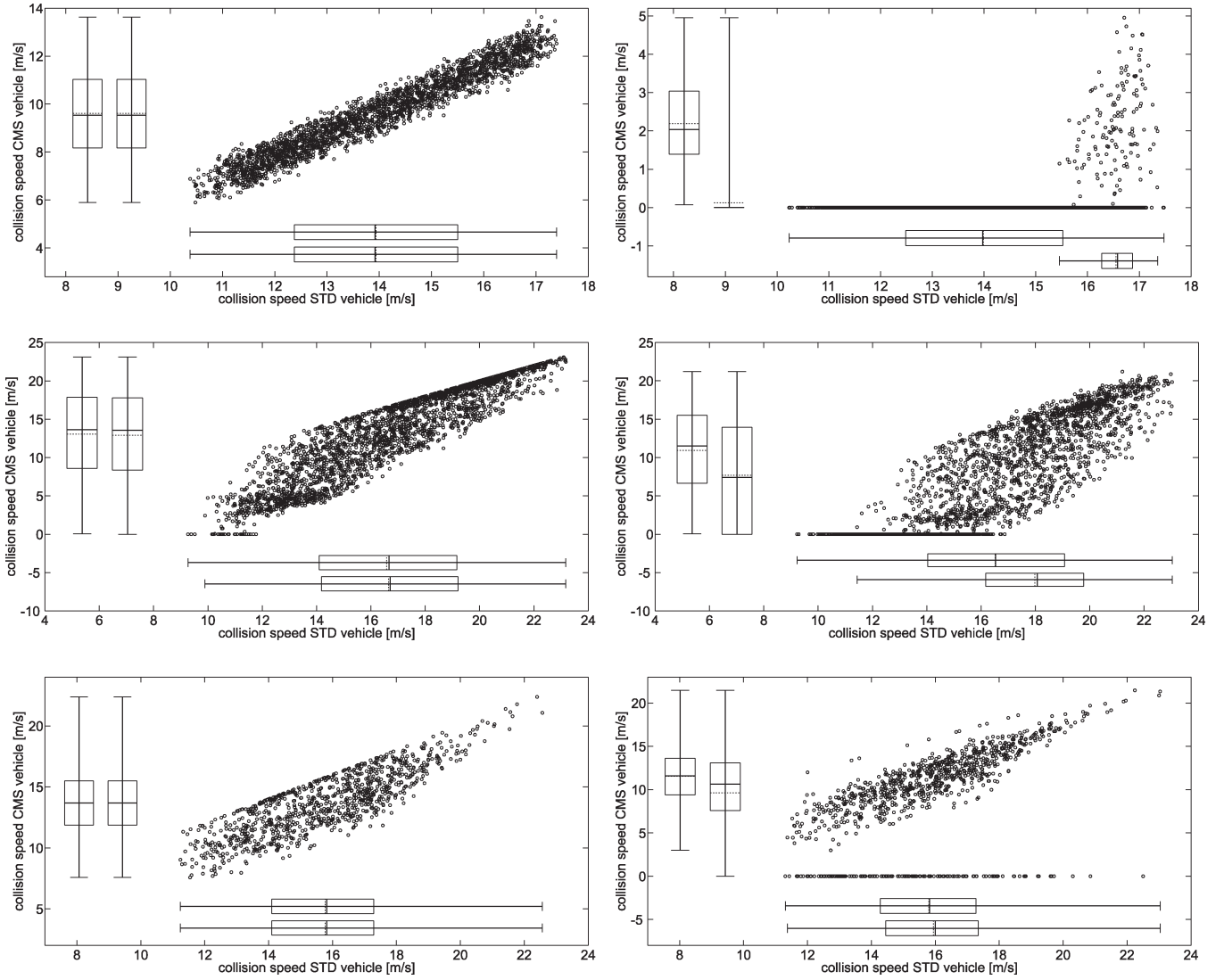


Fig. 11. Scatter plots of the distribution of collision velocities $\Pr(\mathbf{v}_{\text{col}}|\mathbf{S})$ and boxplots of the respective marginals. The outer boxplots correspond to those events where a collision has not been avoided by the CM system, whereas the inner boxplots are based on the whole data set. Rows: Situation classes 1, 2, and 3. Columns: Two-level and three-level CM systems.

exceeds the limit of -4 m/s^2 in the following. Between 0.9 and 1.3 s, the actual deceleration rises to its set value, which yields a smooth transition of TTR_{mod} from 1.1 to 2.4 s. For the next 0.7 s, this situation remains stationary, and TTR_{mod} again falls linearly to -45° , indicating that the situation is getting more critical because the actual deceleration is not sufficient to avoid the collision. At a simulation time of 2.0 s, a jump occurs in the TTR_{mod} signal, which is because the truck vehicle has reached the first half of its lane change maneuver and steers back to reduce its lateral velocity. This change in the object's motion causes TTS_{mod} to fall below TTB_{mod} , which eventually results in the jump in TTR_{mod} through the max operator used in (17). On the other hand, TTR_{max} is not influenced by this change until a simulation time of 2.5 s. From there on, braking is the better alternative to steering, even if the object vehicle tries to "escape" to the left or to the right. At a simulation time of 2.8 s, the activation criteria for the CM system's second level are fulfilled, and the set deceleration equals the required deceleration again. Although the actual deceleration does not reach the set deceleration, the situation

becomes less critical,⁵ and after a simulation time of 3.3 s, a collision is no longer likely to occur, given that the object maintains its state of motion, and the ego vehicle maintains its current deceleration. However, the CM system remains active until a simulation time of 4 s, where the relative speed has been reduced to zero, and no further braking is needed.

B. Stochastic Simulation and Performance Analysis

Two thousand five hundred Monte Carlo runs have been conducted for each situation class and each of the two CMS parameterizations (31) and (35). Table II shows the estimated collision probabilities for each combination of situation class and CMS parameterization. Therein, $\Pr(\bar{\mathbf{C}}, \bar{\mathbf{S}})$ denotes the joint probability that neither the CMS ego vehicle nor the STD ego vehicle collided with the object. $\Pr(\bar{\mathbf{C}}|\mathbf{S})$ refers to the

⁵This is because in our implementation of a_{req} , the object is virtually moved a little closer to the ego vehicle such that a small residual distance is achieved instead of an infinitesimal touching.

conditional probability that the CM system avoided a collision that happened with the STD vehicle. $\Pr(\bar{C}|S)^*$ refers to the same event, with the difference that all those situations in which the reaction time gain ΔTTR was at least 1 s have also been counted as avoided collisions. Although this assumption is somewhat hypothetical, it reflects the fact that a good-conditioned driver should be able to initiate appropriate measures to avoid the collision when provided with an additional second of reaction time. Situations in which “only” the CMS ego vehicle happened to collide with the object vehicle have not been encountered, and a corresponding column has been omitted in Table II.

Concerning the collision probabilities, the differences between both parameterizations are most apparent when looked at situation class 1. The conservatively parameterized two-level CM system neither avoids any collision by itself nor does it provide the driver with a noteworthy gain of reaction time. Its benefit solely restricts to a reduction of collision speed. The three-level CM system, on the contrary, avoids almost 95% of the collisions. Even for the remaining 5% of the situations, it provides enough additional reaction time to the driver, such that a notable avoidance rate of 99% could be achieved. A look at Fig. 11 further points out that even in those cases where a collision has not been avoided, the mean absolute collision velocity is reduced from 16.6 m/s for the STD vehicle to roughly 2.1 m/s for the three-level CMS vehicle.

In contrast to situation class 1, a high amount of collisions are physically inevitable at situation class 2. This is in part due to the fact that a cutting-in maneuver cannot be detected arbitrarily early for the sake of avoiding frequent false alarms. Nevertheless, the avoidance rates for the three-level system are of a respectable magnitude of 30% compared to hardly 4% for the two-level system. Moreover, as shown in Fig. 12, the average collision velocity reduces by 7 m/s (respectively, 9 m/s) for the three-level system compared to 3.5 m/s for the two-level system. Particularly with regard to the rather high collision velocities, every saved “meter per second” improves the chance of survival.

Of all analyzed situation classes, the use case “general intersection” is by far the most challenging one. A look at Table II reveals why: Either a collision does not happen at all (simply because the vehicles miss each other, which is the case in approximately 60% of all simulated intersection scenarios), or the collision will most likely happen regardless of the CM system parameterization. After all, the three-level system still avoids 16.5% of the collisions, but besides some outliers, the reaction time gain is still too small to be of much use for the driver. Nevertheless, the driver benefits from a reduction in collision speed around $\Delta v_{col} = 2.5$ m/s for the two-level system and $\Delta v_{col} = 5$ m/s for the three-level system. For a more comprehensive study of intersection situations, which also considers the case of both vehicles being equipped with the CM system, see [19].

VI. CONCLUSION

In this paper, we presented our concept of a multilevel CM system. We introduced the TTR as a means to assess the criticality of a traffic situation under certainty and outlined algorithms to its efficient computation. Since this metric is tailored to the

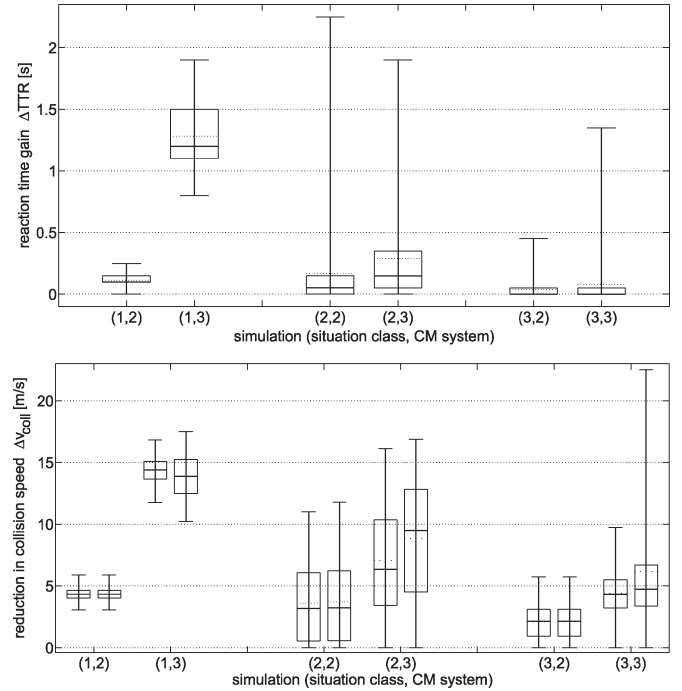


Fig. 12. Upper: Boxplots of the distributions of the reaction time gain $\Pr(\Delta TTR)$. The vertical lines with the crossbars at their ends denote the distribution's support, whereas the horizontal lines of the box represent the interquartile range from the first quartile to the third quartile. The bold and dashed horizontal lines indicate the median and mean, respectively. Lower: Boxplots of the collision speed reductions $\Pr(\Delta v_{col})$. The left boxes of each group correspond to those cases where a collision has not been avoided by the CM system, whereas the right boxes include those cases with $v_{col}^{CMS} = 0$.

driver's possible actions, it builds a suited basis to the problem of decision making in the context of CM system design. The proposed decision-making approach incorporates both sensor and prediction uncertainties and allows for an intuitive tradeoff between potential benefit on the one hand and readiness to take risk with respect to product liability and driver acceptability on the other, while, at the same time, being of manageable complexity.

We further investigated the performance of two differently parameterized CM systems—a rather conservative system with two levels for early braking at low deceleration and late braking at maximum deceleration, respectively, as well as a less restricted system with an additional intermediate level. We looked at three typically dangerous situations, namely rear-end collisions due to the sudden braking of a preceding vehicle, cutting-in vehicles at highway-like speeds, and general intersection situations. The results presented show that an overly conservative CM system sacrifices much of its potential benefit. Unless there is adequate legal certainty concerning product liability, however, system designers may not be able to tap the full potential of these systems. We further conclude that certain traffic situations are inherently difficult to deal with, no matter how ventured the CM system might be parameterized. A simple overtaking scenario can get arbitrary critical if the object suddenly cuts in and a blind spot monitoring or a lane keeping support system at the object vehicle might be the only measure to circumvent these kinds of accidents. The use case of general intersections requires even more advanced technology like infrastructure-based solutions or vehicle-to-vehicle

communication to enhance the environmental perception [20], [21] to avoid accidents with cross traffic on a broader scale or significantly reduce their severity.

REFERENCES

- [1] A. Vahidi and A. Eskandarian, "Research advances in intelligent collision avoidance and adaptive cruise control," *IEEE Trans. Intell. Transp. Syst.*, vol. 4, no. 3, pp. 143–153, Sep. 2003.
- [2] R. Labayrade, C. Royere, and D. Aubert, "A collision mitigation system using laser scanner and stereovision fusion and its assessment," in *Proc. IEEE Intell. Veh. Symp.*, 2005, pp. 441–446.
- [3] A. Polychronopoulos, M. Tsogas, A. Amditis, U. Scheunert, L. Andreone, and F. Tango, "Dynamic situation and threat assessment for collision warning systems: The EUCLIDE approach," in *Proc. IEEE Intell. Veh. Symp.*, 2004, pp. 636–641.
- [4] R. Karlsson, J. Jansson, and F. Gustafsson, "Model-based statistical tracking and decision making for collision avoidance application," in *Proc. Amer. Control Conf.*, 2004, pp. 3435–3440.
- [5] J. Hilgert, K. Hirsch, T. Bertram, and M. Hiller, "Emergency path planning for autonomous vehicles using elastic band theory," in *Proc. IEEE/ASME Int. Conf. Adv. Intell. Mechatronics*, 2003, pp. 1390–1395.
- [6] T. Brandt, T. Sattel, and J. Wallaschek, *On automatic collision avoidance*, 2004. VDI-Berichte.
- [7] A. Bemporad and M. Morari, "Control of systems integrating logic, dynamic, and constraints," *Automatica*, vol. 35, no. 3, pp. 407–427, Mar. 1999.
- [8] A. Broadhurst, S. Baker, and T. Kanade, "Monte Carlo road safety reasoning," in *Proc. IEEE Intell. Veh. Symp.*, 2005, pp. 319–324.
- [9] J. Hillenbrand, V. Schmid, and K. Kroschel, "Situation assessment algorithm for a collision prevention assistant," in *Proc. IEEE Intell. Veh. Symp.*, 2005, pp. 459–465.
- [10] G. Tao, "Adaptive control design and analysis," in *Adaptive and Learning Systems for Signal Processing, Communications, and Control*, 1st ed. Hoboken, NJ: Wiley, 2003.
- [11] R. Kovordányi, K. Ohlsson, and T. Alm, "Dynamically deployed support as a potential solution to negative behavioral adaptation," in *Proc. IEEE Intell. Veh. Symp.*, 2005, pp. 613–618.
- [12] L. Yang, H. Yang, E. Feron, and V. Kulkarni, "Development of a performance-based approach for a rear-end collision warning and avoidance system for automobiles," in *Proc. IEEE Intell. Veh. Symp.*, 2003, pp. 361–321.
- [13] J. Brynielsson and S. Arnborg, "Bayesian games for threat prediction and situation analysis," in *Proc. FUSION*, 2004. [Online]. Available: <http://citeseer.ist.psu.edu/brynielsson04bayesian.html>
- [14] M. A. Goodrich and E. R. Boer, "Designing human-centered automation: Tradeoffs in collision avoidance system design," *IEEE Trans. Intell. Transp. Syst.*, vol. 1, no. 1, pp. 40–54, Mar. 2000.
- [15] I. Dagli, G. Breuel, H. Schittenhelm, and A. Schanz, "Cutting-in vehicle recognition for ACC systems—Towards feasible situation analysis methodologies," in *Proc. IEEE Intell. Veh. Symp.*, 2004, pp. 925–930.
- [16] R. Möbus and U. Kolbe, "Multi-target multi-object tracking sensor fusion of radar and infrared," in *Proc. IEEE Intell. Veh. Symp.*, 2004, pp. 732–737.
- [17] A. Eidehall, T. B. Schön, and F. Gustafsson, "The marginalized particle filter for automotive tracking applications," in *Proc. IEEE Intell. Veh. Symp.*, 2005, pp. 370–375.
- [18] W. Fastenmaier, H. Gсталter, and U. Lehnig, "Analyse von Spurwechselsvorgängen im Verkehr," *Zeitschrift für Arbeitswissenschaft*, vol. 1, 2001.
- [19] J. Hillenbrand and K. Kroschel, "A study on the performance of uncooperative collision mitigation systems at intersection-like traffic situations," in *Proc. IEEE Int. Conf. CIS*, 2006.
- [20] K. Tischler and B. Hummel, "Enhanced environmental perception by inter-vehicle data exchange," in *Proc. IEEE Intell. Veh. Symp.*, 2005, pp. 313–318.
- [21] S. Tsugawa, "Inter-vehicle communications and their applications to intelligent vehicles," in *Proc. IEEE Intell. Veh. Symp.*, 2002, pp. 564–569.



Mr. Hillenbrand received the 2003 Student Prize from the City of Karlsruhe for his Diploma thesis on spectrum pooling systems.

Jörg Hillenbrand (S'04) received the Diploma degree (Dipl.-Ing.) in electrical engineering and information technology from the Universität Karlsruhe, Karlsruhe, Germany, in 2002, where he is currently working toward the Doctoral degree (Dr.-Ing.) in electrical engineering and information technology.

He is currently doing research at DaimlerChrysler, Sindelfingen, Germany. His research interests include wireless communications, sensor fusion, estimation, and intelligent transportation systems, in particular safety-related driver assistance systems.



Andreas M. Spieker received the Diploma degree (Dipl.-Ing.) in technical cybernetics and the Doctoral degree (Dr.-Ing.) from the Universität Stuttgart, Stuttgart, Germany, in 1992 and 2000, respectively.

He was with the Institut für Systemdynamik und Regelungstechnik, Universität Stuttgart. Since 1998, he has been with DaimlerChrysler AG, Sindelfingen, Germany (Group Research), working on advanced driver assistance systems. His research interests include intelligent transportation systems, sensor data fusion, and situation analysis for driver assistance systems.



Kristian Kroschel studied electrical engineering at the University of Erlangen-Nürnberg, Erlangen, Germany, and the University of Karlsruhe, Karlsruhe, Germany, from which he received the Diploma degree in 1967. He received the Ph.D. degree from the University of Karlsruhe in 1971.

Since 1977, he has been a Professor of communication engineering with the Department of Electrical Engineering and Information Technology, University of Karlsruhe. From 1987 to 1991, he headed in parallel the Digital Signal Processing and Diagnosis Group, Fraunhofer Institute of Information and Data Processing, Karlsruhe. He has held the following positions with the Department of Electrical Engineering, University of Karlsruhe: Vice Dean (1982–1983), member of the Administration Board of the University (1984–1992), member of the Senate of the University (1986–1990), and Student Dean (2000–2002). Several times, he was a Visiting Professor with the Technion, Haifa, Israel, the University of California, Santa Barbara, and Bandung Institute of Technology, Bandung, Indonesia. On the field of signal processing and communication, he has authored or coauthored more than 60 papers and three books. His special interest is on signal processing of acoustic and video signals applied to man-machine communication.

Dr. Kroschel is a member of the VDE: the German association of engineers in electrical engineering, electronics, and information technology.